Multimomentum and multiflavor active-sterile neutrino oscillations in the early universe: Role of neutrino asymmetries and effects on nucleosynthesis

Ninetta Saviano,[1,2,3] Alessandro Mirizzi,[1] Ofelia Pisanti,[2,3] Pasquale Dario Serpico,[4]
Gianpiero Mangano,[3] and Gennaro Miele[2,3]

[1]*II Institut für Theoretische Physik, Universität Hamburg, Luruper Chaussee 149, 22761 Hamburg, Germany*
[2]*Dipartimento di Scienze Fisiche, Università di Napoli Federico II, Complesso Universitario di Monte S. Angelo, I-80126 Napoli, Italy*
[3]*Istituto Nazionale di Fisica Nucleare—Sezione di Napoli, Complesso Universitario di Monte S. Angelo, I-80126 Napoli, Italy*
[4]*LAPTh, Université de Savoie, CNRS, B.P.110, Annecy-le-Vieux F-74941, France*

(Received 12 February 2013; published 11 April 2013)

We perform a study of the flavor evolution in the early universe of a multiflavor active-sterile neutrino system with parameters inspired by the short-baseline neutrino anomalies. In a neutrino-symmetric bath a "thermal" population of the sterile state would quickly grow, but in the presence of primordial neutrino asymmetries a self-suppression as well as a resonant sterile neutrino production can take place, depending on temperature and chosen parameters. In order to characterize these effects, we go beyond the usual average momentum and single-mixing approximations and consider a multimomentum and multiflavor treatment of the kinetic equations. We find that the enhancement obtained in this case with respect to the average momentum approximation is significant, up to ~20% of a degree of freedom. Such a detailed and computationally demanding treatment further raises the asymmetry values required to significantly suppress the sterile neutrino production, up to $|L_\nu| \gtrsim \mathcal{O}(10^{-2})$. For such asymmetries, however, the active-sterile flavor conversions happen so late that significant distortions are produced in the electron (anti)neutrino spectra. The larger $|L_\nu|$, the more the impact of these distortions takes over as a dominant cosmological effect, notably increasing the ^{4}He abundance in primordial nucleosynthesis. The standard expression of the primordial yields in terms of the effective number of neutrinos and asymmetries is also greatly altered. We numerically estimate the magnitude of such effects for a few representative cases and comment on the implications for current cosmological measurements.

DOI: 10.1103/PhysRevD.87.073006 PACS numbers: 14.60.St, 14.60.Pq, 26.35.+c, 98.80.−k

I. INTRODUCTION

In recent years different short-baseline neutrino oscillation experiments have found anomalous results that may be interpreted by enlarging the standard description of neutrino oscillations in terms of three active species. In particular, the $\bar{\nu}_\mu \to \bar{\nu}_e$ oscillations in the LSND [1] and MiniBoone [2] experiments (recently constrained by the imaging cosmic and rare underground signals experiment [3]), the $\bar{\nu}_e$ and ν_e disappearance revealed by the reactor anomaly [4], and the gallium Anomaly [5] can be described in terms of light [$m \sim \mathcal{O}(1)$ eV] sterile neutrinos which mix with the active ones (see Refs. [6,7] for recent reviews). In this context, scenarios with one (dubbed "3 + 1") or two ("3 + 2") sterile neutrinos [8–14] have been proposed to fit the different data.

Cosmological measurements represent a powerful tool to probe the number of neutrinos and their mass at eV scale (see, e.g., Refs. [15–17]). The nonelectromagnetic radiation content in the universe is usually expressed in terms of the effective number of excited neutrino species, $N_{\rm eff}$. This can be constrained by cosmic microwave background (CMB) [18–20], large-scale structure (LSS) [19,20], and big bang nucleosynthesis (BBN) data [21–23]. Current measurements, especially CMB ones, slightly favor the existence of some extra radiation, though the results of the WMAP-9 data release [24] and the Atacama Cosmology Telescope [25], when combined with other cosmological constraints, are compatible with the Standard Model expectation value, $N_{\rm eff} = 3.046$ [26]. In particular, WMAP-9 finds $N_{\rm eff} = 3.84 \pm 0.40$ when the full data are analyzed [24], while Atacama gives $N_{\rm eff} = 2.79 \pm 0.56$. In this context, a recent Bayesian analysis of the current cosmological data sets does not show a strong preference for a value of $N_{\rm eff}$ larger than the standard one [27]. Very recently, a combination of cosmological data—notably including the ones released by Planck—has yielded $N_{\rm eff} = 3.30 \pm 0.27$ [28].

Similarly, up to about one fully thermalized sterile neutrino is still marginally allowed by BBN [21,23], while a value corresponding to two sterile states appears largely excluded [29], but there is no significant preference for a larger-than-standard value of $N_{\rm eff}$ either. Notice, however, that even a single extra thermalized sterile neutrino with mass $m \sim \mathcal{O}(1)$ eV appears to be inconsistent with mass bounds from CMB and LSS data [22,30–34].

In order to reconcile the eV sterile neutrino interpretation of the short-baseline anomalies with the cosmological observations, the most straightforward possibility would be to suppress the sterile neutrino thermalization in the early universe, correspondingly reducing the expected excess in extra radiation. In this sense, it was proposed at first in

Ref. [35] (see also Ref. [36]) to consider a primordial asymmetry between neutrinos and antineutrinos,[1]

$$L_\nu = \frac{n_\nu - n_{\bar{\nu}}}{n_\gamma}. \quad (1)$$

In principle, one would expect the neutrino asymmetry to be of the same order of magnitude as the baryonic one, $\eta = (n_B - n_{\bar{B}})/n_\gamma \simeq 6 \times 10^{-10}$. This of course holds for charged leptons, due to the stringent requirement of the charge neutrality of the universe, but not necessarily for neutrinos. In fact, the constrains on L_ν are quite loose, also allowing $|L_\nu| \simeq 10^{-2}$–10^{-1} [38–47]. A primordial neutrino asymmetry would add an additional "matter term potential" in the active-sterile neutrino equations of motion. If sufficiently large, one expects this term to *block* the active-sterile flavor conversions via the in-medium suppression of the mixing angle. Nevertheless, this term can also generate Mikheev-Smirnov-Wolfenstein [48] like resonant flavor conversions among active and sterile neutrinos, *enhancing* their production. In order to assess which of the two effects dominates the flavor evolution it is mandatory to perform a study of the kinetic equations for active-sterile neutrino oscillations.

In a recent paper [49] some of us performed a first study of active-sterile flavor conversions in the presence of neutrino asymmetries, considering (3 + 1) and (2 + 1) scenarios inspired by the recent fits of all the short-baseline neutrino anomalies. In order to simplify the numerical complexity of the problem, we adopted equations of motion integrated over momenta, often referred to as an "average (or single)-momentum approximation." Loosely speaking, this can be thought of as an approximation in which all neutrinos share the common thermal average comoving momentum $\langle p \rangle / T = 3.15$. Under this assumption, we found that in the case of equal asymmetries among the active species, a value of $|L_\nu| \simeq 10^{-3}$ is required to start suppressing the resonant sterile production. An even larger result, $|L_\nu| \simeq 10^{-2}$, is necessary to lower the sterile neutrino abundance in the case of opposite initial asymmetries.

However, $N_{\rm eff}$ is not the only parameter that can affect the cosmological observables. Indeed, for such large values of L_ν resonant active-sterile neutrino conversions occur near or after the decoupling temperature for the active neutrinos, making ineffective the repopulation of active species through collisions. The lack of a repopulation of electron neutrinos would in general produce distorted distributions that can move up the n/p freeze-out and hence increase the ^{4}He yield, the main product of BBN. In order to characterize the possible distortions in the active neutrino spectra, it is necessary to go beyond the average-momentum approximation and consider a detailed treatment of the full momentum-dependent kinetic equations, due to the momentum dependence of the resonant conversions between active and sterile neutrinos.

The purpose of the present work is to perform for the first time a full multiflavor and multimomentum treatment of the active-sterile neutrino oscillations for the (2 + 1) scenario considered in Ref. [49] in the presence of primordial neutrino asymmetries. It was shown in Ref. [49] that this model captures the main features of the complete (3 + 1) scenario. In particular, we follow the evolution of the system in the presence of $|L_\nu| \gtrsim 10^{-3}$, where the distortions of the active neutrino spectra start to become sizable. We remark that for smaller values of the active neutrino asymmetries the thermalization of the sterile neutrinos is complete, producing a tension with cosmological data. In the studied cases, we observed an enhancement in the sterile neutrino production of up to $\Delta N_{\rm eff} \simeq 0.2$ with respect to that observed in the average-momentum study [49]. This implies that one needs to consider even larger asymmetries (at least of the order of $|L_\nu| \sim 10^{-2}$) in order to significantly suppress the production of sterile neutrinos. On the other hand, for these values of the asymmetries we find relevant distortions in the electron (anti)neutrino spectra, notably modifying the BBN yields (see, e.g., Refs. [50,51]). Reliably computing these distortions and $N_{\rm eff}$ as functions of the asymmetry parameters is a very challenging task, involving time-consuming numerical calculations for the flavor evolution. Nonetheless, the few representative values of the asymmetries we investigated already allow one to draw nontrivial implications for cosmological observables.

This article is structured as follows. In Sec. II we briefly summarize our formalism, highlighting the modifications with respect to Ref. [49]. We present our results concerning the sterile neutrino production in the multimomentum scenario and the differences with respect to the average-momentum case. Then, in Sec. III we show the distortion of the electron neutrino spectra for different values of asymmetries and we discuss the impact on observables, namely $N_{\rm eff}$ and ^{4}He and ^{2}H abundances. Finally, in Sec. IV we conclude.

II. MULTIMOMENTUM FLAVOR EVOLUTION

A. Equations of motion

In this section we summarize the equations of motion (EoMs) for the (2 + 1) active-sterile neutrino system in the early universe, using the same notation as Ref. [49], to which we address the reader for details. In particular, we describe the time evolution of the neutrino ensemble in terms of the following dimensionless variables (replacing time, momentum, and photon temperature, respectively):

$$x \equiv ma, \qquad y \equiv pa, \qquad z \equiv T_\gamma a, \quad (2)$$

where m is an arbitrary mass scale which we put equal to the electron mass m_e. Note that the function a is normalized, without loss of generality, so that $a(t) \to 1/T$ at large

[1]Alternative escape routes have been recently proposed; see, e.g., Ref. [37].

temperatures, T being the common temperature of the particles in equilibrium far from any entropy-release process. With this choice, a^{-1} can be identified with the initial temperature of thermal, active neutrinos.

In order to take into account the interplay between oscillations and collisions of neutrinos, it is necessary to describe the neutrino (antineutrino) system in terms of 3×3 density matrices ϱ ($\bar{\varrho}$),[2]

$$\varrho(x, y) = \begin{pmatrix} \varrho_{ee} & \varrho_{e\mu} & \varrho_{es} \\ \varrho_{\mu e} & \varrho_{\mu\mu} & \varrho_{\mu s} \\ \varrho_{se} & \varrho_{s\mu} & \varrho_{ss} \end{pmatrix}. \tag{3}$$

In this formalism we write the EoMs for ϱ and $\bar{\varrho}$ as [38,52,53]

$$i\frac{d\varrho}{dx} = +\frac{x^2}{2m^2 y\bar{H}}[\mathsf{M}^2, \varrho] + \frac{\sqrt{2}G_F m^2}{x^2\bar{H}} \times \left[\left(-\frac{8ym^2}{3x^2m_W^2}\mathsf{E}_\ell - \frac{8ym^2}{3x^2m_Z^2}\mathsf{E}_\nu + \mathsf{N}_\nu\right), \varrho\right] + \frac{x\hat{C}[\varrho]}{m\bar{H}}, \tag{4}$$

$$i\frac{d\bar{\varrho}}{dx} = -\frac{x^2}{2m^2 y\bar{H}}[\mathsf{M}^2, \bar{\varrho}] + \frac{\sqrt{2}G_F m^2}{x^2\bar{H}} \times \left[\left(+\frac{8ym^2}{3x^2m_W^2}\mathsf{E}_\ell + \frac{8ym^2}{3x^2m_Z^2}\mathsf{E}_\nu + \mathsf{N}_\nu\right), \bar{\varrho}\right] + \frac{x\hat{C}[\bar{\varrho}]}{m\bar{H}}, \tag{5}$$

which has to be solved along with the covariant conservation of the total stress-energy tensor,

$$x\frac{d\varepsilon}{dx} = \varepsilon - 3\mathcal{P}. \tag{6}$$

In the previous expressions $\bar{H}$ denotes the properly normalized Hubble parameter,

$$\bar{H} \equiv \frac{x^2}{m}H = \frac{x^2}{m}\sqrt{\frac{8\pi\epsilon(x, z(x))}{3M_{\rm Pl}^2}} = \left(\frac{m}{M_{\rm Pl}}\right)\sqrt{\frac{8\pi\varepsilon(x, z(x))}{3}}, \tag{7}$$

and the total energy density and pressure enter through their "comoving transformed" values $\varepsilon \equiv \epsilon(x/m)^4 \simeq \varepsilon_\gamma + \varepsilon_e + \varepsilon_\nu$ and $\mathcal{P} \equiv P(x/m)^4$. Compared with the treatment in Ref. [49], we now take into account the nonrelativistic transition of the electrons and the entropy transfer to the photons, which is responsible for increasing the temperature of photons with respect to the one of neutrinos, i.e., for making $z(x) > 1$. However, since we are only interested in situations where the change with respect to the instantaneous decoupling limit value $N_{\rm eff} = 3$ is much larger than the $\sim$1.5% effect due to incomplete neutrino decoupling during $e^+ - e^-$ annihilation [26], we neglect the latter effect. We can thus track $z(x)$ once and for all by using the integrated entropy ratio formula [see, e.g., Eq., (15) in Ref. [54], with df_i/dx at the right-hand side put to zero].

The first term on the right-hand side of Eqs. (4) and (5) accounts for vacuum oscillations, where in the flavor basis $\mathsf{M}^2 = \mathcal{U}^\dagger\mathcal{M}^2\mathcal{U}$. Here $\mathcal{U} = \mathcal{U}(\theta_{e\mu}, \theta_{es}, \theta_{\mu s})$ is the 3×3 active-sterile mixing matrix, parametrized as in Ref. [49]. We assume $\theta_{e\mu}$ is equal to the active 1–3 mixing angle θ_{13} [55], while we fix the active-sterile mixing angles to the best-fit values of the different anomalies [10],

$$\sin^2\theta_{e\mu} = 0.024, \tag{8}$$

$$\sin^2\theta_{es} = 0.025, \tag{9}$$

$$\sin^2\theta_{\mu s} = 0.023. \tag{10}$$

The mass-squared matrix $\mathcal{M}^2 = \mathrm{diag}(-\Delta m^2_{\rm atm}/2, +\Delta m^2_{\rm atm}/2, \Delta m^2_{\rm st})$ is parametrized in terms of the atmospheric mass-squared difference $\Delta m^2_{\rm atm} = 2.43 \times 10^{-3}\ \mathrm{eV}^2$ [55] and of the active-sterile mass splitting $\Delta m^2_{\rm st} = 0.89\ \mathrm{eV}^2$, fixed from the short-baseline fit in the $3 + 1$ model [10]. In the following we assume the normal mass hierarchy $\Delta m^2_{\rm atm} > 0$. We checked that results similar to the ones we will present would have been obtained considering the $(2 + 1)$ sub-sector associated with the solar mass-squared difference $\Delta m^2_{\rm sol}$ and with the 1–2 mixing angle θ_{12}.

The terms proportional to G_F in Eqs. (4) and (5) encode the matter effects in the neutrino oscillations. In particular, the term E_ℓ is related to the energy density of electrons and positrons [see Eq. (20) in Ref. [49]], while the $\nu - \nu$ interaction terms are given by

$$\mathsf{N}_\nu = \frac{1}{2\pi^2}\int dy y^2\{\mathsf{G}_s(\varrho(x, y) - \bar{\varrho}(x, y))\mathsf{G}_s + \mathsf{G}_s\,\mathrm{Tr}[(\varrho(x, y) - \bar{\varrho}(x, y))\mathsf{G}_s]\}, \tag{11}$$

$$\mathsf{E}_\nu = \frac{1}{2\pi^2}\int dy y^3\mathsf{G}_s(\varrho(x, y) + \bar{\varrho}(x, y))\mathsf{G}_s. \tag{12}$$

Note that the matrix N_ν is related to the *difference* of the density matrices of neutrinos and antineutrinos, while E_ν is related to their sum. The matrix $\mathsf{G}_s = \mathrm{diag}(1, 1, 0)$ in flavor space contains the dimensionless coupling constants. We remark that when considering more than one active species, the N_ν matrix also contains off-diagonal terms. In the presence of large neutrino asymmetries among the active species, such as the ones we are considering in this work, the matter effects are dominated by the N_ν contribution. This latter term makes the EoMs nonlinear and are the main numerical challenge in dealing with this physical system. At large temperatures it dominates over the vacuum term, suppressing any flavor conversions. However, as the universe expands a *resonance* condition can be satisfied at lower temperatures, as extensively illustrated in Ref. [49].

[2]Here ν_μ refers generically to a nonelectron active flavor state.

Finally, the last term in Eqs. (4) and (5) is the collisional one proportional to G_F^2, for which we adopt the same approximate expression $\hat{C}[\rho]$ as in Eq. (28) of Ref. [49], but now keeping the y dependence (see Ref. [56]). This guarantees that (i) the correct collisional term is recovered when integrating the EoMs for $\varrho(y)$ over momenta, and (ii) the overall lepton-number conservation is preserved. Note that this is not the case for alternative damping prescriptions often found in the literature, where the lepton-number conservation is achieved by imposing an additional equation (see, e.g., Ref. [57]). We remark that possible minor inaccuracies in the y dependence of the collisional terms are of little concern for our application, since in the cases where large spectral distortions are produced in the electron (anti)neutrino distributions, these are caused by oscillatory terms rather than collisional ones. In other words, whenever the collisional repopulation of depleted active neutrinos is relevant, one has very little departures from thermal spectra, while in the opposite limit the major distortion is not due to the exact y dependence of the collisional terms. On the other hand, implementing an operator enforcing lepton-number conservation (numerically to a very high degree of precision) is crucial to avoid spurious numerical effects.

In order to fix the initial conditions for the flavor evolution, we notice that active neutrinos are produced in the very early universe with their energy spectrum kept in chemical and kinetic equilibrium by weak interactions until temperatures $T \simeq$ few MeV, when the corresponding collision rates fall below the cosmological expansion rate. In the presence of primordial neutrino asymmetries, the original active neutrino spectra are given by Fermi-Dirac distributions parametrized in terms of a temperature T_ν and chemical potentials μ_α for $\alpha = e,\ \mu,\ \tau$. Each neutrino asymmetry in Eq. (1) can be expressed in terms of the corresponding degeneracy parameter $\xi_\alpha = \mu_\alpha/T_\nu$ as

$$L_\alpha = \frac{1}{12\zeta(3)}\left(\frac{T_\nu}{T_\gamma}\right)^3(\pi^2\xi_\alpha + \xi_\alpha^3) \simeq 0.68\xi_\alpha\left(\frac{T_\nu}{T_\gamma}\right)^3, \qquad (13)$$

with $\zeta(3) \simeq 1.202$, where the right-hand numerical expression corresponds to the leading order in small ξ_α. In the rest of the paper, we shall indicate the neutrino asymmetries in terms of the ξ_α parameters rather than L_α, in order to conform with the more frequently used notation in phenomenological papers.

The initial conditions for the density matrix ϱ are then given by

$$\begin{aligned}\varrho_{\rm in} &= {\rm diag}(f_{\rm eq}(y, \xi_e), f_{\rm eq}(y, \xi_\mu), 0),\\ \bar{\varrho}_{\rm in} &= {\rm diag}(f_{\rm eq}(y, -\xi_e), f_{\rm eq}(y, -\xi_\mu), 0),\end{aligned} \qquad (14)$$

with $f_{\rm eq}(y, \xi) = 1/[\exp(y - \xi) + 1]$.

We remark that since in our study we consider initial distributions for active neutrinos close to their equilibrium ones,[3] the oscillations among the three active species have a qualitatively important role, but quantitatively their details are of minor relevance for the evolution of the sterile neutrinos. Therefore, the (2 + 1) scenario we consider is a good proxy for the complete (3 + 1) scenario. We also mention that in a recent work [58], a multimomentum study was performed of the kinetic equations for a system consisting of only one active and one sterile neutrino species [i.e., (1 + 1) scenario]. While instructive in several respects, this is quite a simplified scenario since it does not allow one to incorporate effects, like the existence of more than one active-sterile mixing angle and different choices of the neutrino asymmetries for the different flavors.

B. Results

In this section we present our results for the sterile neutrino abundance in the (2 + 1) scenario described in Sec. II A. We numerically solve the EoMs (4) and (5) with an integration routine for stiff ordinary differential equations taken from the NAG libraries [59] and based on an adaptive method. The range for x is chosen to be $x \in [2 \times 10^{-2}, 0.5]$. As a compromise between the energy resolution of the spectral distortions and computational cost, we took $N_y = 21$ momentum modes in the range $y \in [0, 10]$. The grid points are not chosen to be equally spaced, but are instead fixed by imposing a weighted Gaussian quadrature of the integrals on the right-hand side of Eqs. (11) and (12). By increasing the momentum grid points to $N_y = 30$, we checked in some test runs that this is enough to keep the error below the percent level on the effective number of neutrinos $N_{\rm eff}$.

We remark that due to the momentum dependence of the resonance conditions, in the multimomentum treatment of the EoMs there can be significant deviations with respect to the evolution predicted by the average-momentum scheme. A direct comparison between the single-momentum and the multimomentum results is reported in Fig. 1, which shows (a) the momentum-integrated sterile neutrino density matrix element (solid curves) normalized to the integral of a Fermi-Dirac distribution with zero chemical potential,

$$\rho_{ss}(x) = \frac{\int dy y^2 \varrho_{ss}(x, y)}{\int dy y^2 f_{\rm eq}(y, 0)}, \qquad (15)$$

and (b) the sterile neutrino density matrix element ρ_{ss} in the average-momentum scheme (dot-dashed curves), normalized correspondingly. In the left panels we take equal initial neutrino asymmetries, $\xi_e = \xi_\mu$, while in the right panels we refer to opposite ones, $\xi_e = -\xi_\mu$. In the upper panels we consider $\xi_e = 10^{-3}$, while in the lower panels we take

[3]This is conservative since some population of sterile neutrinos cannot be excluded in extensions of the Standard Model, following, for example, from decays of heavier neutrino singlet states.

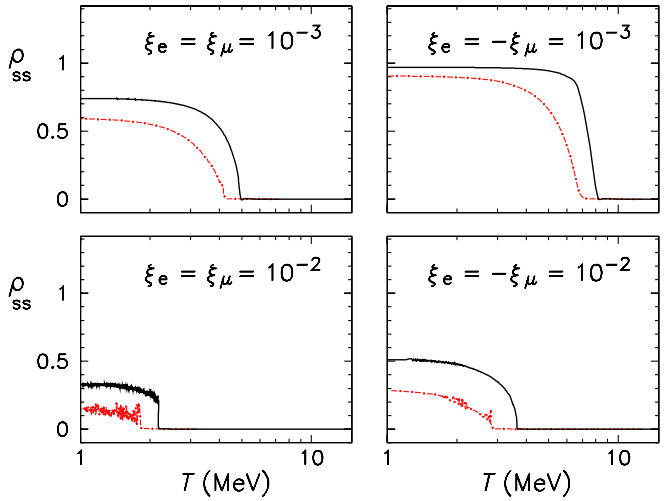

FIG. 1 (color online). Evolution of the total value of the sterile neutrino density matrix element ρ_{ss} as a function of the temperature T for the multimomentum case (continuous curves) and the average-momentum (dot-dashed curves) case with a thermal momentum $\langle y \rangle = 3.15$. Left panels correspond to $\xi_e = \xi_\mu$, while in the lower panels $\xi_e = -\xi_\mu$. Upper panels refer to $\xi_e = 10^{-3}$ and right panels to $\xi_e = 10^{-2}$.

$\xi_e = 10^{-2}$. In all the considered cases the values of ρ_{ss} for the single momentum underestimates the sterile neutrino abundance with respect to the multimomentum case. The enhancement obtained with the multimomentum treatment is significant, roughly $\sim$20% of a degree of freedom. Moreover, we note that the sterile production in the multimomentum case occurs at higher temperatures with respect to the average-momentum case. This is due to the fact that in the multimomentum evolution the sterile neutrino population can start building up earlier via lower momenta modes that resonate earlier than the average momentum. This anticipates the dynamical evolution of ξ and is the main factor responsible for the difference observed. Also, we confirm the observation of Ref. [60] that the resonance is more adiabatic at higher temperatures. Hence, the average-momentum treatment of the EoMs is generically expected to *underestimate* the sterile neutrino abundance.

III. IMPACT ON OBSERVABLES: $N_{\rm eff}$ AND LIGHT-NUCLEI ABUNDANCES

Phenomenological quantities affected by active-sterile neutrino flavor conversions notably depend on the overall nonelectromagnetic radiation content, parametrized via $N_{\rm eff}$, and from the distortions of the electron (anti)neutrino spectra, the latter being a basic input for BBN weak rates.[4]

[4]Actually, properly treating effects that are sensitive to the neutrino masses requires knowing the flavor composition of the neutrino ensemble as well. Similarly, precision computations of CMB anisotropies are in principle sensitive to the neutrino phase-space distributions; see, e.g., Ref. [61].

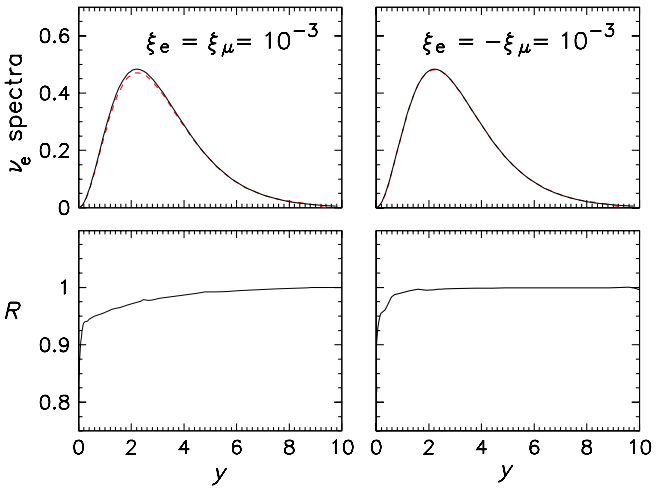

FIG. 2 (color online). Cases with $\xi_e = 10^{-3}$. *Upper panels*: Final ν_e energy spectra at $T = 1$ MeV (dashed curve) and initial ones (continuous curve). *Lower panel*: Ratio R between final and initial ν_e energy spectra. Left panels refer to $\xi_e = \xi_\mu$ while right panels are for $\xi_e = -\xi_\mu$.

In the upper panels of Figs. 2 and 3 we show the y-dependent ν_e energy spectrum $y^2 \varrho_{ee}(y)$ (dashed curve) at $T = 1$ MeV, compared with the initial one $y^2 f_{\rm eq}(y, \xi_e)$ (solid line). In particular, Fig. 2 refers to $\xi_e = 10^{-3}$ and Fig. 3 to $\xi_e = 10^{-2}$. In each figure, in the left panels $\xi_e = \xi_\mu$, while in the right ones $\xi_e = -\xi_\mu$. In order to characterize the distortion in the ν_e spectra with respect to the initial one, in the lower panel we plot the ratio

$$R = \frac{\varrho_{ee}(y)}{f_{\rm eq}(y, \xi_e)}. \tag{16}$$

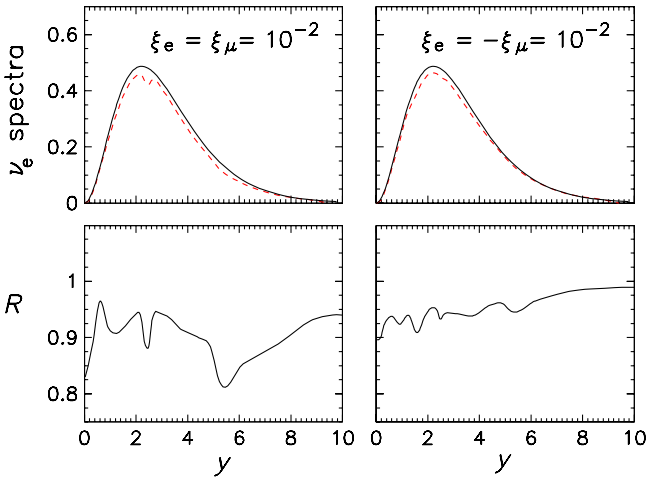

FIG. 3 (color online). Cases with $\xi_e = 10^{-2}$. *Upper panels*: Final ν_e energy spectra at $T = 1$ MeV (dashed curve) and initial ones (continuous curve). *Lower panel*: Ratio R between final and initial ν_e energy spectra. Left panels refer to $\xi_e = \xi_\mu$ while right panels are for $\xi_e = -\xi_\mu$.

In the case of $\xi_e = 10^{-3}$, $R \gtrsim 0.95$ for equal asymmetries and $R \gtrsim 0.98$ in the case of opposite asymmetries. Conversely, the spectral distortions are more evident for $\xi_e = 10^{-2}$. Namely, for equal asymmetries one finds $R \gtrsim 0.82$, while for opposite asymmetries $R \gtrsim 0.9$. Indeed, spectral distortions in the active neutrinos are more evident when resonant active-sterile conversions occur near the active neutrino decoupling temperature, as pointed out first in Ref. [62].

We recall that, as already mentioned in Ref. [49], the dynamical evolution of the asymmetries is such that *both* neutrinos and antineutrinos get populated resonantly, roughly in equal values. Hence, we only show here the results referring to neutrinos. Of course, in the numerical computation the small differences between the two sectors have been properly accounted for.

Concerning the effective number of neutrino species, we remark that at the level of approximation we are adopting, $N_{\rm eff} = 3 + \Delta N_{\rm eff}$ enters the dynamics only via its contribution to the Hubble parameter [see Eq. (7)], where it rescales the standard neutrino energy density contribution ε_ν as

$$\varepsilon_\nu(x, N_{\rm eff}) \rightarrow \varepsilon_\nu(x, 3)\left(1 + \frac{\Delta N_{\rm eff}}{3}\right). \tag{17}$$

Technically, we compute $\Delta N_{\rm eff}$ in the above equation via the following (numerical) integral:

$$\Delta N_{\rm eff} = \frac{60}{7\pi^4}\int dy y^3\, {\rm Tr}[\varrho(x, y) + \bar{\varrho}(x, y)] - 2, \tag{18}$$

the factor "-2" being due to the fact that we are considering only two active neutrino species.

The quantity defined in Eq. (18) is shown in Fig. 4 for two representative values of asymmetries ($\xi_e = 10^{-3}$ for solid curves and $\xi_e = 10^{-2}$ for dashed curves), taken to be equal (opposite) for the e and μ sector in the left (right) panel. For $\xi_e = 10^{-3}$, we see that the resonant production of sterile neutrinos starts around $T \simeq 5$ MeV for equal asymmetries and $T \simeq 8$ MeV for opposite ones. Since active-sterile neutrino conversions mostly occur when the collisional regime is still operative, the active neutrino

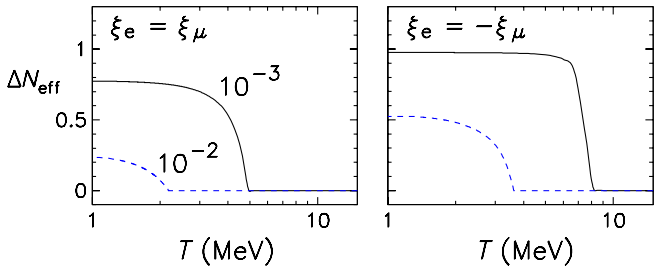

FIG. 4 (color online). Evolution of $\Delta N_{\rm eff}$ vs temperature T for equal asymmetries $\xi_e = \xi_\mu$ (left panel) and opposite asymmetries $\xi_e = -\xi_\mu$ (right panel). Solid curves refer to $\xi_e = 10^{-3}$ while dashed curves are for $\xi_e = 10^{-2}$.

TABLE I. The values of $\Delta N_{\rm eff}$ and the calculated abundances of the ^{4}He mass fraction Y_p and deuterium ^{2}H in the different cases considered in this paper. For comparison, the third column refers to the increase in the effective degrees of freedom obtained in the average-momentum approximation, $\Delta N_{\rm eff}^{\langle y\rangle}$.

Case	$\Delta N_{\rm eff}$	$\Delta N_{\rm eff}^{\langle y\rangle}$	Y_p	^{2}H/H($\times 10^5$)
$\lvert\xi\rvert \ll 10^{-3}$	1.0	1.0	0.259	2.90
$\xi_e = -\xi_\mu = 10^{-3}$	0.98	0.89	0.257	2.87
$\xi_e = \xi_\mu = 10^{-3}$	0.77	0.51	0.256	2.81
$\xi_e = -\xi_\mu = 10^{-2}$	0.52	0.44	0.255	2.74
$\xi_e = \xi_\mu = 10^{-2}$	0.22	0.04	0.251	2.64
$\xi_e = \lvert\xi_\mu\rvert = 10^{-3}$, no ν_s	$\sim$0	$\cdots$	0.246	2.56
$\xi_e = \lvert\xi_\mu\rvert = 10^{-2}$, no ν_s	$\sim$0	$\cdots$	0.244	2.55
Standard BBN	0	0	0.247	2.56

species are almost fully repopulated, reflected in a $\Delta N_{\rm eff} \simeq \rho_{ss}$ in both cases (see Fig. 1). This is still true to some extent for the case $\xi_e = -\xi_\mu = 10^{-2}$, but not when $\xi_e = \xi_\mu = 10^{-2}$. Namely, in this latter situation, the resonant population starts at temperatures as low as $T \sim 2$ MeV, comparable to the neutrino decoupling temperature. This means that active neutrino repopulation is only partial. Also, an appreciable difference (in this case of $\sim$0.1) is established between ρ_{ss} and $N_{\rm eff}$. These effects were already noted in Ref. [49], where they were even more prominent due to the "less effective" sterile production associated to the single-momentum approximation.

The numerical values of the $\Delta N_{\rm eff}$'s found in a few representative runs are reported in Table I along with the values of the yields of the ^{4}He mass fraction Y_p and deuterium ^{2}H, as obtained from a modified version of the numerical code PARTHENOPE [63] for a baryon fraction $\omega_b = 0.02249$ and the neutron lifetime $\tau_n = 880.1$ s, following Particle Data Group 2012 recommendations [64]. For comparison, we also show cases with neutrino asymmetries but no sterile neutrinos, as well as the standard BBN case.

Technically, note that the rates $\Gamma_{n\rightarrow p}[f_{\nu_e}, f_{\bar{\nu}_e}]$ and $\Gamma_{p\rightarrow n}[f_{\nu_e}, f_{\bar{\nu}_e}]$ are functionals of the distributions f_{ν_e}, $f_{\bar{\nu}_e}$. If we denote with Γ^0 the rates computed in the Born approximation for Fermi-Dirac spectra and with Γ the actual rates for the cases at hand, we have computed the effect of sterile neutrinos by rescaling the rates implemented in the code PARTHENOPE [63] (see also Ref. [65]) by Γ/Γ^0, which has been numerically evaluated and then interpolated. This amounts to a first-order correction in a perturbative approach. However, since the rate corrections are at most $\mathcal{O}(3\%)$ for the largest asymmetries, the error due to this approximation is safely below 0.3% (see, e.g., Ref. [66] for the analysis of corrections to Born weak rates). Thus, this is comparable or lower than neglecting the modification to the reheating in the standard scenario. In determining the shape of the distribution function, especially for the cases with $\lvert\xi\rvert = 10^{-2}$, the main source of

error in fact comes from the discretization of the neutrino distribution (and the corresponding interpolation). Still, test runs with an $N_y = 30$ points grid in momentum space suggest that this does not spoil the reliability of the size of the effects we found.

With reference to Table I, a few comments are in order. First, note that for sufficiently small values of $\xi_{e,\mu}$, all effects of sterile states on BBN is due to the increased $N_{\rm eff}$, which is in any case larger than that found in the single-momentum approximation for the same value of $|\xi|$. This holds true for both Y_p and ^{2}H. On the other hand, for high values, say $|\xi_{e,\mu}| \sim 10^{-2}$, some fraction of the sterile neutrino population builds up relatively late, namely *after* the freeze-out of the active neutrinos. These cases are associated to a $\Delta N_{\rm eff}$ significantly smaller than 1. While this quantity is still the main cause of the change in ^{2}H, a significant fraction of the effect on Y_p is due to the changes of the weak rates regulating the $n \leftrightarrow p$ chemical equilibrium due to distorted ν_e and $\bar{\nu}_e$ distributions. In the case $\xi_e = -\xi_\mu = 10^{-2}$, this effect is $\sim$75% than the one related to the speed-up of the expansion due to $\Delta N_{\rm eff}$, while for $\xi_e = \xi_\mu = 10^{-2}$ it becomes three times larger than the other.[5] Phenomenologically, these scenarios with large asymmetries in the presence of sterile neutrinos yield comparatively lower values of $N_{\rm eff}$ as probed by CMB (say, $N_{\rm eff} \simeq 3.2$), while altering Y_p by an amount loosely equivalent to a larger $N_{\rm eff}$. We note that in these cases the presence of eV sterile neutrinos pushes the change of Y_p in the direction of an *increase* with respect to the standard BBN value. This behavior confirms the prediction based on analytical estimations presented in Ref. [67]. The comparison with the last three rows in Table I also shows that this trend is *opposite* of that obtained in the presence of a positive-sign electron neutrino asymmetry (in the absence of sterile neutrinos). Actually, in some previous phenomenological analyses that did not treat sterile neutrinos dynamically (like in Ref. [22]) the possibility "to mask" the presence of extra eV-scale sterile neutrino degrees of freedom to BBN has been envisaged by introducing large chemical potentials, treating the system as a "degenerate BBN" plus extra radiation. This prescription may lead to even *qualitatively wrong* conclusions, such as the positive correlation in allowed regions between the increase of ξ and $N_{\rm eff}$, visible, e.g., in Fig. 6 of Ref. [22].

Quantitatively, we observe that the modifications of BBN yields induced by sterile neutrinos are sizable, as reported in Table I. For comparison, the statistical error on the astrophysical Y_p determination can be as small as 0.001 (albeit the systematic error is at the moment several times larger) [68], the determination of ^{2}H/H in the highest quality quasar system is $(2.535 \pm 0.05) \times 10^{-5}$ [23], and the 1σ errors on $N_{\rm eff}$ and Y_p reported by the combined analysis of the Planck team amount to $\Delta N_{\rm eff} \simeq 0.27$ and $\Delta Y_p \simeq 0.021$ [28], in substantial agreement with earlier forecasts [69].

Finally, we checked that by changing squared-mass differences and mixing angles within current uncertainties [70] one can easily obtain $\mathcal{O}(10\%)$ differences in $N_{\rm eff}$. Also, the results presented here are rather on the conservative side, as far as the chosen particle mass parameter. For example, considering only disappearance experiments, values of the sterile mass splitting larger than the 0.89 eV^2 used here are preferred; see e.g., Ref. [71]. In this case, the results we obtained are modified in the sense of an easier thermalization of the sterile state.

IV. CONCLUSIONS

In this paper, we have presented for the first time the results of a multiflavor, multimomentum computation of cosmological neutrino spectra in the presence of a sterile state with parameters consistent with those invoked in the interpretations of short-baseline neutrino oscillation experiments [10]. We have considered the case of relatively large neutrino asymmetries ($|L_\nu| \gtrsim 10^{-3}$–10^{-2}), which suppress the sterile production in the early universe, giving in this way a better agreement with several cosmological observations. Our results show an enhancement in the sterile neutrino abundance of up to 0.2 effective degrees of freedom with respect to that observed in the average-momentum study. This shifts the asymmetries needed for a significant suppression of $N_{\rm eff}$ to relatively larger values, of the order of $|L_\nu| \gtrsim 10^{-2}$. Moreover, starting with opposite asymmetries in different flavors with vanishing net neutrino asymmetries provides a less effective inhibition. On the other hand, for large asymmetries the significant production of the sterile neutrinos after the ν_e and $\bar{\nu}_e$ decoupling causes non-negligible distortions (from a few percent up to $\sim$20% for some of the cases considered) in the ν_e and $\bar{\nu}_e$ energy distributions. As a result—leaving aside the problem of how to generate such large initial asymmetries—the modifications of BBN yields are sizable, as reported in Table I. Also worth noting is that—while for ^{2}H/H these modifications are essentially due to the larger $N_{\rm eff}$—for the ^{4}He mass fraction Y_p a significant effect follows from (anti)neutrino distribution distortions produced in the presence of both asymmetries and a sterile state.

Although it is not the purpose of the present paper to provide cosmological constraints on sterile neutrinos, we can outline the following two possible scenarios:

(i) The thermalization of the sterile state in the presence of small or vanishing neutrino asymmetries: In the "interesting" parameter space this is often close to

[5]The evolution for this latter case is extremely slow and there is still a small evolution in the parameters taking place at $T \lesssim 1$ MeV. Hence the results presented here, which assume that the asymptotic results are equal to the ones at the smallest temperatures followed, are slightly *conservative*. The actual effect should be a bit larger.

total, and already with pre-Planck data tensions were manifest between cosmologically disfavored regions and laboratory claims (see, e.g., Fig. 5 in Ref. [72] or the left panel of Fig. 3 in Ref. [33]). This is amenable to a systematic analysis of the sterile neutrino mass and mixing parameter space, and a first analysis following the Planck data release is strengthening the above-mentioned tensions [73].

(ii) No complete thermalization of sterile neutrinos: Extra ingredients (which imply major cosmological changes) must be introduced. The most popular proposal in the literature has been to invoke neutrino asymmetries, whose effects on cosmological observables has been treated with simplified recipes. Here we put this possibility under close scrutiny, finding notable differences with naive expectations found in the literature. This scenario could lead to a possible inconsistency in the value of $N_{\rm eff}$ extracted from CMB and BBN. Indeed, sterile neutrinos and large asymmetries would produce a relatively low value of $N_{\rm eff}$ as probed by CMB, and an increase of Y_p. This latter would be mimicked by a *larger* $N_{\rm eff}$. It is also worth stressing that the standard BBN prediction $Y_p = Y_p(\omega_b, N_{\rm eff})$ *is not valid anymore*. Given our current CPU power, we have limited our analysis of this scenario to a few representative cases. Contrary to what is proposed in the scenario (i), a large scan over parameter space (which would be needed for a quantitative statistical analysis combining CMB, LSS, and BBN data) appears to be a hard task. Indeed, any precise quantitative result for the cosmological observables would depend on an interplay of active-active and active-sterile neutrino oscillations (multiflavor effects), whose matrix structure is not fully determined by current data on short-baseline neutrino anomalies (most notably in the $\tau - s$ sector). Hence "precision" computations would be illusory and premature, given the dependence from unknown or poorly constrained parameters.

Future directions of these studies would depend on the fate of the short-baseline neutrino anomalies and on the current generation of cosmological measurements. Definitely, these results are already orienting—and will orient even more in the near future—further research on the nontrivial role played by light sterile neutrinos in cosmology.

ACKNOWLEDGMENTS

We thank Carlo Giunti for providing us with preliminary results from new fits of the short-baseline neutrino data. We acknowledge Irene Tamborra for a careful reading of the draft and for useful comments on it. The work of A. M. and N. S. was supported by the German Science Foundation (DFG) within the Collaborative Research Center 676 "Particles, Strings and the Early Universe." G. Mangano, G. Miele, and O. P. acknowledge support by the *Istituto Nazionale di Fisica Nucleare* I. S. FA51 and the PRIN 2010 "Fisica Astroparticellare: Neutrini ed Universo Primordiale" of the Italian *Ministero dell'Istruzione, Università e Ricerca*. G. Miele and O. P. acknowledge partial support by Progetto FARO 2010 of the University of Naples Federico II. At LAPTh, this activity was developed coherently with the research axes supported by the excellence laboratory (Labex) grant ENIGMASS.

[1] A. Aguilar-Arevalo *et al.* (LSND Collaboration), Phys. Rev. D **64**, 112007 (2001).
[2] A. A. Aguilar-Arevalo *et al.* (The MiniBooNE Collaboration), Phys. Rev. Lett. **105**, 181801 (2010).
[3] M. Antonello *et al.*, arXiv:1209.0122.
[4] G. Mention, M. Fechner, T. Lasserre, T. A. Mueller, D. Lhuillier, M. Cribier, and A. Letourneau, Phys. Rev. D **83**, 073006 (2011).
[5] M. A. Acero, C. Giunti, and M. Laveder, Phys. Rev. D **78**, 073009 (2008).
[6] K. N. Abazajian *et al.*, arXiv:1204.5379.
[7] A. Palazzo, arXiv:1302.1102.
[8] E. Akhmedov and T. Schwetz, J. High Energy Phys. 10 (2010) 115.
[9] J. Kopp, M. Maltoni, and T. Schwetz, Phys. Rev. Lett. **107**, 091801 (2011).
[10] C. Giunti and M. Laveder, Phys. Rev. D **84**, 073008 (2011).
[11] C. Giunti and M. Laveder, Phys. Rev. D **84**, 093006 (2011).
[12] A. Donini, P. Hernandez, J. Lopez-Pavon, M. Maltoni, and T. Schwetz, J. High Energy Phys. 07 (2012) 161.
[13] C. Giunti, M. Laveder, Y. F. Li, Q. Y. Liu, and H. W. Long, Phys. Rev. D **86**, 113014 (2012).
[14] J. Kopp, P. A. N. Machado, M. Maltoni, and T. Schwetz, arXiv:1303.3011.
[15] J. Lesgourgues and S. Pastor, Phys. Rep. **429**, 307 (2006).
[16] Y. Y. Y. Wong, Annu. Rev. Nucl. Part. Sci. **61**, 69 (2011).
[17] S. Riemer-Sorensen, D. Parkinson, and T. M. Davis, arXiv:1301.7102.
[18] E. Komatsu *et al.* (WMAP Collaboration), Astrophys. J. Suppl. Ser. **192**, 18 (2011).
[19] Z. Hou, R. Keisler, L. Knox, M. Millea, and C. Reichardt, arXiv:1104.2333.
[20] S. Das *et al.*, Astrophys. J. **729**, 62 (2011).
[21] G. Mangano and P. D. Serpico, Phys. Lett. B **701**, 296 (2011).

[22] J. Hamann, S. Hannestad, G. G. Raffelt, and Y. Y. Y. Wong, J. Cosmol. Astropart. Phys. 09 (2011) 034.
[23] M. Pettini and R. Cooke, arXiv:1205.3785.
[24] G. Hinshaw *et al.*, arXiv:1212.5226.
[25] J. L. Sievers *et al.*, arXiv:1301.0824.
[26] G. Mangano, G. Miele, S. Pastor, T. Pinto, O. Pisanti, and P. D. Serpico, Nucl. Phys. **B729**, 221 (2005).
[27] S. Feeney, H. V. Peirisa, and L. Verde, arXiv:1302.0014.
[28] P. A. R. Ade *et al.* (Planck Collaboration), arXiv:1303.5076.
[29] T. D. Jacques, L. M. Krauss, and C. Lunardini, arXiv:1301.3119.
[30] J. Hamann, S. Hannestad, G. G. Raffelt, I. Tamborra, and Y. Y. Y. Wong, Phys. Rev. Lett. **105**, 181301 (2010).
[31] M. C. Gonzalez-Garcia, M. Maltoni, and J. Salvado, J. High Energy Phys. 08 (2010) 117.
[32] S. Riemer-Sorensen, D. Parkinson, T. M. Davis, and C. Blake, Astrophys. J. **763**, 89 (2013).
[33] M. Archidiacono, N. Fornengo, C. Giunti, and A. Melchiorri, Phys. Rev. D **86**, 065028 (2012).
[34] S. Joudaki, K. N. Abazajian, and M. Kaplinghat, Phys. Rev. D **87**, 065003 (2013).
[35] R. Foot and R. R. Volkas, Phys. Rev. Lett. **75**, 4350 (1995).
[36] Y.-Z. Chu and M. Cirelli, Phys. Rev. D **74**, 085015 (2006).
[37] C. M. Ho and R. J. Scherrer, Phys. Rev. D **87**, 065016 (2013).
[38] A. D. Dolgov, S. H. Hansen, S. Pastor, S. T. Petcov, G. G. Raffelt, and D. V. Semikoz, Nucl. Phys. **B632**, 363 (2002).
[39] Y. Y. Y. Wong, Phys. Rev. D **66**, 025015 (2002).
[40] K. N. Abazajian, J. F. Beacom, and N. F. Bell, Phys. Rev. D **66**, 013008 (2002).
[41] P. D. Serpico and G. G. Raffelt, Phys. Rev. D **71**, 127301 (2005).
[42] S. Pastor, T. Pinto, and G. G. Raffelt, Phys. Rev. Lett. **102**, 241302 (2009).
[43] M. Shimon, N. J. Miller, C. T. Kishimoto, C. J. Smith, G. M. Fuller, and B. G. Keating, J. Cosmol. Astropart. Phys. 05 (2010) 037.
[44] G. Mangano, G. Miele, S. Pastor, O. Pisanti, and S. Sarikas, J. Cosmol. Astropart. Phys. 03 (2011) 035.
[45] E. Di Valentino, M. Lattanzi, G. Mangano, A. Melchiorri, and P. Serpico, Phys. Rev. D **85**, 043511 (2012).
[46] G. Mangano, G. Miele, S. Pastor, O. Pisanti, and S. Sarikas, Phys. Lett. B **708**, 1 (2012).
[47] E. Castorina, U. Franca, M. Lattanzi, J. Lesgourgues, G. Mangano, A. Melchiorri, and S. Pastor, Phys. Rev. D **86**, 023517 (2012).
[48] L. Wolfenstein, Phys. Rev. D **17**, 2369 (1978); S. P. Mikheev and A. Y. Smirnov, Yad. Fiz. **42**, 1441 (1985) [Sov. J. Nucl. Phys. **42**, 913 (1985)].
[49] A. Mirizzi, N. Saviano, G. Miele, and P. D. Serpico, Phys. Rev. D **86**, 053009 (2012).
[50] D. P. Kirilova and M. V. Chizhov, Phys. Lett. B **393**, 375 (1997).
[51] D. P. Kirilova and M. V. Chizhov, Nucl. Phys. **B534**, 447 (1998).
[52] B. H. J. McKellar and M. J. Thomson, Phys. Rev. D **49**, 2710 (1994).
[53] G. Sigl and G. Raffelt, Nucl. Phys. **B406**, 423 (1993).
[54] S. Esposito, G. Miele, S. Pastor, M. Peloso, and O. Pisanti, Nucl. Phys. **B590**, 539 (2000).
[55] G. L. Fogli, E. Lisi, A. Marrone, D. Montanino, A. Palazzo, and A. M. Rotunno, Phys. Rev. D **86**, 013012 (2012).
[56] N. F. Bell, R. R. Volkas, and Y. Y. Y. Wong, Phys. Rev. D **59**, 113001 (1999).
[57] K. Enqvist, K. Kainulainen, and J. Maalampi, Nucl. Phys. **B349**, 754 (1991).
[58] S. Hannestad, I. Tamborra, and T. Tram, J. Cosmol. Astropart. Phys. 07 (2012) 025.
[59] http://www.nag.co.uk/numeric/numerical_libraries.asp.
[60] P. Di Bari and R. Foot, Phys. Rev. D **65**, 045003 (2002).
[61] J. Lesgourgues and T. Tram, J. Cosmol. Astropart. Phys. 09 (2011) 032.
[62] K. Abazajian, N. F. Bell, G. M. Fuller, and Y. Y. Y. Wong, Phys. Rev. D **72**, 063004 (2005).
[63] O. Pisanti, A. Cirillo, S. Esposito, F. Iocco, G. Mangano, G. Miele, and P. D. Serpico, Comput. Phys. Commun. **178**, 956 (2008).
[64] J. Beringer *et al.* (Particle Data Group Collaboration), Phys. Rev. D **86**, 010001 (2012).
[65] P. D. Serpico, S. Esposito, F. Iocco, G. Mangano, G. Miele, and O. Pisanti, J. Cosmol. Astropart. Phys. 12 (2004) 010.
[66] S. Esposito, G. Mangano, G. Miele, and O. Pisanti, Nucl. Phys. **B540**, 3 (1999).
[67] C. J. Smith, G. M. Fuller, C. T. Kishimoto, and K. N. Abazajian, Phys. Rev. D **74**, 085008 (2006).
[68] Y. I. Izotov and T. X. Thuan, Astrophys. J. **710**, L67 (2010).
[69] L. Perotto, J. Lesgourgues, S. Hannestad, H. Tu, and Y. Y. Y. Wong, J. Cosmol. Astropart. Phys. 10 (2006) 013.
[70] C. Giunti (private communication).
[71] C. Giunti, M. Laveder, Y. F. Li, and H. W. Long, Phys. Rev. D **87**, 013004 (2013).
[72] A. Melchiorri, O. Mena, S. Palomares-Ruiz, S. Pascoli, A. Slosar, and M. Sorel, J. Cosmol. Astropart. Phys. 01 (2009) 036.
[73] A. Mirizzi, G. Mangano, N. Saviano, E. Borriello, C. Giunti, G. Miele, and O. Pisanti, arXiv:1303.5368.